Effects of Fractal Trajectory on Gas Diffusion in Porous Media

Baoquan Zhang and Xiufeng Liu
School of Chemical Engineering and Technology & State Key Laboratory of C_1 Chemistry and Technology, Tianjin University, Tianjin 300072, China

A mathematical model was developed to represent the effect of tortuous trajectory and irregular step length on gas diffusion in porous media, and then it was conformed by analyzing the experimentally determined flux with respect to 19 groups of binary gas mixtures in a porous catalyst pellet. Based on the analysis of actual diffusing distance within porous media, the diffusing trajectory of gas molecules was characterized into fractal curves, leading to a novel flux equation of binary gas mixtures. The established model represented the tortuous structure by the only model parameter the fractal dimension of diffusion trajectories d_F. A yardstick was devised to account for the influence of pore size, diffusing species, temperature and pressure on the trajectory length of gas diffusion. The size of the yardstick δ could be found after diffusing species, temperature and pressure were specified for a given porous medium. The fitting between the experimentally determined flux and the model equation resulted in a fractal dimension of 1.102. It was evident that the model prediction was in fairly good agreement between the experimental results in the literature and those of the study, and the irregular degree of diffusing trajectory is much less than that of the pore surface. Detailed comparison with the traditional treatment by the tortuosity factor demonstrated that the methodology established here would be especially significant for very tortuous pore systems.

Introduction

Diffusion is one of the most ubiquitous phenomena in nature. Gas diffusion in porous media is of particular importance to a variety of disciplines because the overall rate of processes may be decisively influenced by diffusive mass transfer (Karger, 2002). The prediction of gas diffusion in porous media is one of the fundamental problems in adsorption, membrane-, and solid-catalyzed reaction processes. A number of publications have shown that many physical and physicochemical processes that occur in porous media are significantly influenced by the porous structure, including both the topology of the pore network and the morphology of the pores (Sahimi et al., 1990; Hollewand and Gladden, 1992; Coppens and Froment, 1995a,b; Mougin et al., 1996 a; Cussler, 1997; Sheintuch, 1999, 2000). For a membrane- or solid-catalyzed reaction, molecules diffuse through the pore network, collide with other molecules or pore walls, and react at active sites on the pore surface. Thereupon, the topology of the pore network and the morphology of the pores influence the lumped performance of diffusion and simultaneous reaction in porous catalysts. On the other hand, the interaction between diffusion and reaction can be large and dramatic, which depends on the ratio of the two individual speeds. The overall rate is closely related to the porous structure in nature (Hollewand and Gladden, 1992; Cussler, 1997; Fogler, 1999).

There are two categories of models for describing diffusion and reaction in porous catalysts: continuum models and network models. Continuum models included a porous catalyst pellet as a continuum with porous space. The gas diffusion in this "porous continuum" was described by using the effective diffusion coefficient in Fick's law. In this "effective" way of treatment, pores were commonly assumed to be straight

Correspondence concerning this article should be addressed to B. Q. Zhang.

cylinders (Hollewand and Gladden, 1992; Coppens and Froment, 1994). As for network models, the topology of the pore network was taken into account, but in almost all published articles the morphology of individual pores was still supposed to be Euclidean for the purpose of simplification in simulations. Until now, only a few articles have dealt with diffusion, or diffusion and simultaneous reaction in porous catalysts including the morphology of the pore and/or its surface (Michaels, 1959; Scott and Dullien, 1962; Eldridge and Brown, 1976; Nakano et al., 1987; Coppens and Froment, 1994; Sheintuch, 1999, 2000; Malek and Coppens, 2001; Sapoval, 2001).

Fractal geometry has been utilized widely to characterize the irregular morphology of natural and artificial objects for the two decades since it was introduced (Mandelbrot, 1983; Avnir, 1989). Analytical and numerical investigations of diffusion and reaction in porous fractal catalysts have shown that mass fractals differ in their behaviors from pore fractals. One unique behavior of diffusion and reaction in pore fractals is the existence of an intermediate low-slope asymptote (Sheintuch and Brandon, 1989; Giona et al., 1996; Mougin et al., 1996b; Gavrilov and Sheintuch, 1997; Sheintuch, 1999, 2000). In the intermediate domain the fractal–catalyst activity is higher than that of the porous catalyst of uniform pores having similar porosity and surface area. The qualitative and quantitative differences between fractal- and uniform-pore catalysts gave rise to the conclusion that the concentration field, the reaction and deactivation rates, as well as selectivity should be remarkably different in those two catalysts. In a series of publications by Coppens and Froment (1994, 1995 a,b, 1996), the irregular pore surface and tortuous pore axis were both taken into consideration, where the fractal analyses together with interpretation of the experimental data in the literature showed that the pore morphology had a strong influence on diffusion and reaction in porous fractal catalysts. From this they reached the conclusion that Fick's first law has to be modified to account for the pore tortuosity in porous catalysts, except that the fractal pore axis is being employed.

Traditionally, the tortuous degree was accounted for by a parameter called the tortuosity factor in the effective diffusion coefficient (Satterfield, 1970; Cussler, 1997; Fogler, 1999). Up to now, many theoretical and experimental investigations have revealed that the tortuosity factor of porous catalysts is related to many factors, such as the topology of the pore network, the morphology of the pores, diffusion species, operational temperature and pressure conditions, and even the Thiele modulus (Hollewand and Gladden, 1992; Coppens and Froment, 1994, 1995b; Zhang, 2001). The experimentally and theoretically determined values of tortuosity factors are very scattered (Satterfield, 1970; Hollewand and Gladden, 1992; Cussler, 1997). It was almost impossible to clarify the physical significance of the tortuosity factor, because it lumped too many influencing factors. Therefore, it was often considered as an empirical parameter and was determined by measuring diffusion flux for various species and then finding the average. This method was only an approximation treatment. In short, the tortuosity factor is not an ideal parameter to represent the tortuous degree of the pores with regard to diffusion in porous media (Coppens and Froment, 1995a).

Whatever model (either a continuum model or a network model) is being used to describe diffusion in porous media, quantitative characterization of the irregularity of the pore shape is a prerequisite. Unfortunately, so far there is very limited information on this aspect, especially from the experimental point of view. The scope of the present study is to develop a mathematical model based on fractal geometry to predict gas diffusion of binary systems in porous catalysts. The fractal dimension of the diffusion trajectory will be used to account for the tortuous degree of the pores with regard to gas diffusion across the whole catalyst pellet, in order to replace the empirical tortuosity factor. As the only model parameter here, the fractal dimension is a measure of the tortuous degree of the pore structure with respect to gas diffusion, and its value should be in the range of $1 \le d_F < 2$. The actual pore length of gas diffusion traversed by different molecules is going to be measured by means of corresponding yardstick sizes related to both the properties of gas mixtures and the pore-size distribution. The validity of the proposed methodology will be examined by detailed comparison with experimental data. Here, the existence of fractal trajectory with respect to gas diffusion in porous media will be verified by both theoretical and experimental investigations.

Mathematical Model

Mean free path and yardstick size of measuring pore length

According to the kinetic theory of statistical thermodynamics, a collision takes place when one molecule moves into the local force field of another molecule. The average distance that molecules travel between collisions is called the "mean free path". It is the average step length, if molecules are imagined to jump in steps. The mean free path is related to many variables, such as the properties of molecules, and the temperature and composition of the system. Once the mean free path and the density of molecules are known, the coefficients of momentum, heat, and mass transfer can be estimated in terms of kinetic theory (Tien and Lienhard, 1979).

Besides the basic kinetic hypothesis for ideal gases, the idealization of molecular size is also assumed here. If the molecules are considered as spherical with diameter σ, when a mixture of ideal gases consists of n species and all molecules move about with a Maxwellian velocity distribution, then the mean free path of the jth species is expressed as (Tien and Lienhard, 1979)

$$\lambda_j = \frac{1}{\pi \sum_i \left(n_i \sigma_{ji}^2 \sqrt{M_j/M_i + 1} \right)} \tag{1}$$

where

$$n_i = \frac{p_i}{k_B T} = \frac{y_i P}{k_B T}$$

and

$$\sigma_{ji} = (\sigma_j + \sigma_i)/2$$

For a binary gas mixture of species A and B, Eq. 1 is reduced to

$$\lambda_A = \frac{k_B T}{\sqrt{2}\, y_A P \pi \sigma_A^2 + y_B P \pi \sigma_{AB}^2 \sqrt{1 + M_A/M_B}} \tag{2}$$

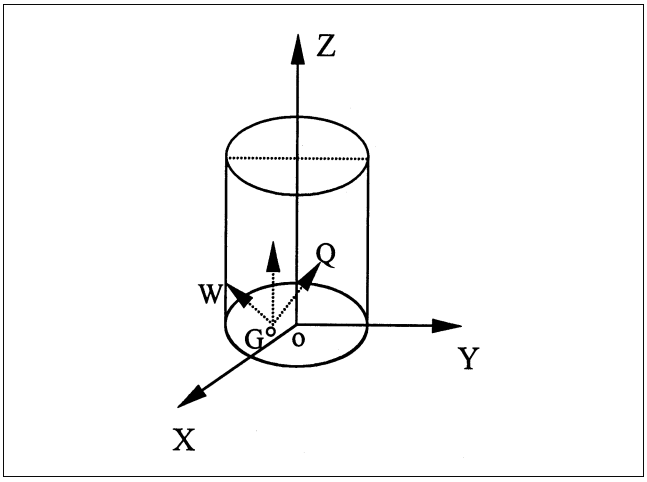

Figure 1. The boundary that molecules can reach at each step of walking under the restriction of the pore wall.

Consider a gas mixture that is in steady axial motion in a cylindrical pore and put the system into the circular cylindrical coordinates, as shown in Figure 1. The molecules collide with either another molecule or the pore wall that keeps the molecules inside the pore. The moving direction of a molecule is altered after it collides with another molecule or the pore wall. The molecules colliding with the pore wall are momentarily adsorbed and then escape from the wall surface in random directions. Suppose a molecule is at position G at an instant of time, it can move in a straight line until it encounters either the pore wall at a point such as W or another molecule at a point such as Q. Both the same species and different species molecules collide with each other (Jackson, 1977).

Momentum transfer is accompanied when collisions between molecules or between a molecule and the pore wall occur. A given species may lose its momentum in the axial direction by (1) direct transfer to the pore wall due to molecule–wall collisions, (2) transfer to another species resulting from collisions between different species of molecules, or (3) indirect transfer to the pore wall by way of a sequence of molecule-molecule collisions terminating in a molecule–wall collision. The flux relations can be deduced according to each of these mechanisms of momentum transfer via pressure-drop calculations (Jackson, 1977). What most concerns us here is not the momentum transfer but the average step length, named the yardstick size, to be utilized to measure the actual pore length when a molecule diffuses through the pore.

Let us imagine that the molecules jump through the pore like hard balls bouncing along a tube. The average step length between each collision within a pore depends on both the mean free path and the pore structure, as stated earlier. For a given porous medium, the pore structure is certain, and, in this case, the average step length changes with the mean free path of the molecule. As shown in the next section, if the pores of porous media are characterized by a set of fractal curves, the length of the pore varies with the yardstick size used for length measurement. Hence, both the mean free path of involved species and the characteristics of the porous catalyst used influence the result of pore-length measurement with respect to gas diffusion. The tortuous structure of a porous catalyst can be quantified by a fractal scaling relation.

Suppose the radius of the pore is r, then in the circular cylindrical coordinates the pore's inner surface can be mathematically described by

$$X^2 + Y^2 = r^2 \tag{3}$$

Assume that one molecule of species A is in the position of $G(X_0,Y_0,0)$. Before the next collision occurs, the trace surface that the molecule could reach without the obstruction of the pore wall would be spherical, which is mathematically expressed by the following equation

$$(X - X_0)^2 + (Y - Y_0)^2 + Z^2 = \lambda_A^2 \tag{4}$$

Because of the existence of the pore wall, the volume surrounded by the two curved surfaces just determined is the space the molecule may reach before a new collision with another molecule or the pore wall happens. The average step length from the point G can be calculated by way of this enclosed space, that is

$$\delta_G = \sqrt[3]{3V/2\pi} \tag{5}$$

where V is the enclosed volume, which can be calculated by the integral equation as follows

$$V = \iiint_V dV = \iint_S \sqrt{\lambda_A^2 - (X - X_0)^2 - (Y - Y_0)^2}\; dX\, dY \tag{6}$$

It is worth noting here δ_G is only the average step length with regard to point G, that is, a point average. If the entire point on the same cross section is considered, the average step length should be the average over the summation of the average step lengths at all the possible points on the cross section of radius r, that is, a cross sectional average. It should be

$$\delta_A = \frac{1}{\pi r^2} \iint_S \delta_G\; dX_0\; dY_0 \tag{7}$$

This is the cross-sectional average step length. As for the porous media with a uniformly distributed pore size, this will be the total average step length throughout the pore system. As shown in the next subsection, δ_A is going to be used to measure the actual length of the pore when the molecules of species A diffuse through the pore bathed in the gas mixture of A and B, leading to a new flux relation.

The assumption of cylindrical pores needs to be tested for its validity. Recently, Sapoval et al. (2001) used the concept of active zone to model the diffusion and reaction in porous catalysts. Their findings indicate that the effect of the irregular geometry of pores is to modify the effective reactivity, but not the diffusion transport coefficient. Furthermore, the effect of pore surface roughness on self- and transport diffu-

sion in porous media in the Knudsen regime was studied by means of dynamic Monte Carlo simulations in three-dimensional (3-D) rough pores (Malek and Coppens, 2001). They reached the conclusion that transport diffusion (the diffusion under the influence of a concentration gradient) in rough pores should be related to the concentration gradient over the pore and the average pore cross section, but not the wall surface irregularity. Thus, the assumption of cylindrical pores is reasonable. And the calculation based on the average pore diameter is also acceptable because of the close relevancy of gas diffusion to the average pore cross section.

Diffusion flux along fractal trajectories in porous media

For binary gas mixtures, when temperature and pressure are uniform everywhere, the diffusion flux of component A along a single pore can be quantified by (Johnson and Stewart, 1965)

$$N_{Ap} = -\frac{1}{\beta}\frac{P}{R_g T}\frac{dy_A}{dL} \tag{8}$$

where

$$\beta = \left[\frac{1 + y_A\left(\sqrt{M_A/M_B} - 1\right)}{D_{AB}} + \frac{1}{D_{KA}}\right]$$

As described earlier, the trajectory of a molecule's walk in the pore zig zags, and the average step length depends on both the pore structure and the mean free path of the molecules. So the actual pore length traversed by different molecules should be different if the average step length is employed as the yardstick size, leading to the argument that the pore length of porous media should be of *fractal* with respect to gas diffusion. Thus, the jumping trajectory of the gas molecules in the pore is represented here by a fractal curve, which is the average over a bunch of curves that indicate all the individual channels inside the porous medium. The fractal dimension of the curve is used to describe the tortuous degree of the jumping trajectory of gas diffusion. Based on dimensional analysis, the curve's fractal length, L (or actual length traversed by gas molecules), and the corresponding Euclidean length, L_0, are merged into (Mandelbrot, 1983; Zhang and Li, 1995)

$$L = L_0^{d_F}\delta^{1-d_F} \tag{9}$$

where δ is the yardstick size measuring the length of the fractal curve, d_F is the fractal dimension, and L_0 is the corresponding projection of the fractal curve. Because the pores inside porous catalysts are connected to each other like a web, this fractal dimension is the average one over all the pores.

If the yardstick size with respect to species A is used to measure the diffusion distance, the fractal length in Eq. 8 must be replaced by Eq. 9, thus transformed into

$$N_{Ap} = -\frac{1}{\beta}\frac{P}{R_g T d_F \delta_A^{1-d_F} L_0^{d_F-1}}\frac{dy_A}{dL_0} \tag{10}$$

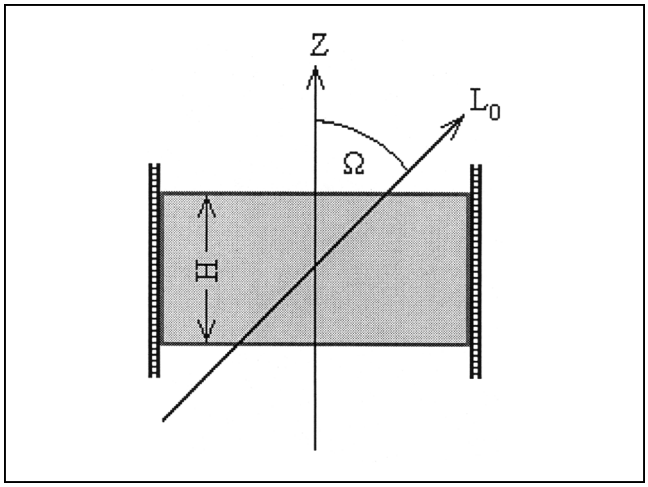

Figure 2. The coordinate plane of catalyst particle.

Put the catalyst pellet into the rectangular coordinates, as shown in Figure 2. Using the ordinate Z instead of L_0, Eq. 10 becomes

$$\frac{(N_{Az})_p}{\cos\Omega} = -\frac{1}{\beta}\frac{P}{R_g T d_F \delta_A^{1-d_F}(Z/\cos\Omega)^{d_F-1}}\frac{dy_A}{d(Z/\cos\Omega)} \tag{11}$$

The transformation and rearrangement of Eq. 11 leads to

$$(N_{AZ})_p = -\frac{P\cos^{d_F+1}\Omega}{\beta R_g T d_F \delta_A^{1-d_F} Z^{d_F-1}}\frac{dy_A}{dZ} \tag{12}$$

The diffusion flux through the whole pellet can be calculated by way of the pore distribution function, which is defined as the void fraction of the main network pores per unit interval of pore size, r, and orientation, Ω The overall flux through the pellet is found by integrating the flux in individual pores (Johnson and Stewart, 1965; Feng and Stewart, 1973)

$$N_{AZ} = \int_0^\infty \int_0^{\pi/2} (N_{AZ})_p f(r,\Omega)\, dr\, d\Omega \tag{13}$$

where $f(r,\Omega)$ is the pore distribution function. If the porous structure is isotropic, the pore distribution function has nothing to do with the orientation of pores, and therefore it only varies with the pore radius, that is, $f(r,\Omega) = f(r)$. Then the term-by-term integration of Eq. 13 gives rise to the following equations for binary mixtures

$$N_{AZ} = \frac{B_{\pi/2}(d_F) P D_{AB}}{R_g T\left(\sqrt{M_A/M_B} - 1\right) H^{d_F}} \int_{r_{\min}}^{r_{\max}} \delta_A^{d_F-1} f(r) Q\, dr$$

$$M_A \neq M_B \quad (14a)$$

$$N_{AZ} = \frac{B_{\pi/2}(d_F) P (y_{A0} - y_{AH})}{R_g T H^{d_F}} \int_{r_{\min}}^{r_{\max}} \frac{\delta_A^{d_F-1} f(r)\, dr}{1/D_{AB} + 1/D_{AK}}$$

$$M_A = M_B, \quad (14b)$$

where

$$B_{\pi/2}(d_F) = \int_0^{\pi/2} \cos^{d_F+1}\Omega \; d\Omega$$

and

$$Q = \ln\left[\frac{1 + y_{A0}\left(\sqrt{M_A/M_B} - 1\right) + D_{AB}/D_{KA}}{1 + y_{AH}\left(\sqrt{M_A/M_B} - 1\right) + D_{AB}/D_{KA}}\right]$$

If the pore size is uniform throughout the whole pellet, the final flux equation based on fractal representation is established as follows

$$N_{AZ} = \frac{B_{\pi/2}(d_F) P D_{AB} \epsilon \overline{Q}}{R_g T\left(\sqrt{M_A/M_B} - 1\right) H} \cdot \left(\frac{\delta_A}{H}\right)^{d_F - 1} \qquad M_A \neq M_B \tag{15a}$$

$$N_{AZ} = \frac{B_{\pi/2}(d_F) P \epsilon (y_{A0} - y_{AH})}{R_g T\left(1/D_{AB} + 1/\overline{D}_{KA}\right) H} \cdot \left(\frac{\delta_A}{H}\right)^{d_F - 1} \qquad M_A = M_B \tag{15b}$$

where (δ_A/H) is a dimensionless yardstick size. It is expected that Eq. 15 can result in a reasonable prediction if the pellet has a narrow pore-size distribution. Otherwise, the effect of pore-size distribution has to be taken into account. For the sake of simplification in nonlinear fitting of Eq. 15 with experimental data, let

$$F_A = \frac{N_{AZ} R_g T\left(\sqrt{M_A/M_B} - 1\right)}{P D_{AB} \epsilon \overline{Q}} \cdot \delta_A \qquad M_A \neq M_B \tag{16a}$$

and

$$F_A = \frac{N_{Az} R_g T\left(1/D_{AB} + 1\overline{D}_{KA}\right)}{P \epsilon (y_{A0} - y_{AH})} \cdot \delta_A \qquad M_A = M_B \tag{16b}$$

Here quantity F is a dimensionless flux of diffusion. So Eqs. 16a and 16b can be changed into the scaling relation that combines the fractal dimension of the diffusion trajectory, the dimensionless yardstick size, and the dimensionless flux of diffusion

$$F_A = B_{\pi/2}(d_F) \cdot (\delta_A/H)^{d_F} \tag{17}$$

The quantity $B_{\pi/2}(d_F)$ virtually acts as an average orientation factor, according to its definition in Eq. 14. But it differs from the classic treatment proposed by Johnson and Stewart (1965) in that it included the influence of the curved structure of the pores. The logarithmic form of the equation is procured by taking the logarithm on the two sides of Eq. 17

$$\ln F_A = d_F \ln(\delta_A/H) + B \tag{18}$$

where quantity $B = \ln B_{\pi/2}(d_F)$.

The fitting of Eq. 17 or 18 can be undertaken in terms of experimentally measured diffusion flux for binary gas mixtures. For a given porous medium, if the pore system is isotropic, the yardstick size for each species of binary gas mixture can be estimated by using Eq. 7 after the mean free path and the average pore size are known, where the average pore diameter is reckoned by the pore-size distribution of the medium. It should be noted here that the use of the yardstick size with regard to the average pore size will only work for narrowly distributed monodisperse porous systems. Furthermore, the dimensionless flux of diffusion is determined from Eq. 16, in which the experimentally measured flux and concentration difference of each run are needed, with the exception of quantities like pressure and temperature, porosity, molecular weights, and the yardstick size.

Also, both the molecular diffusion coefficient and Knudsen diffusion coefficient are required in order to get the dimensionless flux. The molecular diffusion coefficient was estimated with the Chapman-Enskog theory (Cussler, 1997). The Knudsen diffusion coefficient was calculated by (Cunningham and Williams, 1980)

$$D_K = \frac{4d}{3} \cdot \left(\frac{R_g T}{2\pi M}\right)^{1/2} \tag{19}$$

After the dimensionless flux and the corresponding yardstick size have been determined, the fractal dimension of gas diffusion trajectories, the only model parameter, can be obtained by fitting Eq. 16. The quantity $B_{\pi/2}(d_F)$ is also related to the fractal dimension, so this has to be considered in the fitting. The detailed procedure will be presented later in this article.

Experimental

Experimental setups

In order to check the proposed flux equation of diffusion established earlier, experimental setups were established to present reliable data with detailed information of the catalyst pellet, binary gas mixtures, as well as operational variables. Figure 3 shows the flow sheet of the experimental setups. The diffusion cell was separated into two compartments by the molded pellet. The function of the two back-pressure regulators (BPR) was to make the pressure in the two separated compartments constant. The pressure was monitored by a low-pressure gauge. A U-tube manometer was used to show the pressure difference between the two compartments. The system was adjusted to reach equal pressure between the two compartments before any experiment was performed. The diffusion cell was put into a gas chromatographic oven, the temperature of which was controlled by a built-in temperature-detecting and -controlling unit. Two six-port manual valves were used to take samples of the upper and lower compartments and to inject the samples one at a time into the 3380 Varian gas chromatograph. As shown in Figure 3, the carrier gas traveled through the two six-port valves in series. The sample tubes (fixed amount of sample gas) of two six-port valves were both being loaded in this position, that is, the gas effluents from the two compartments passed through the sample tubes separately. The sample gas could be injected into the gas chromatograph by switching the cor-

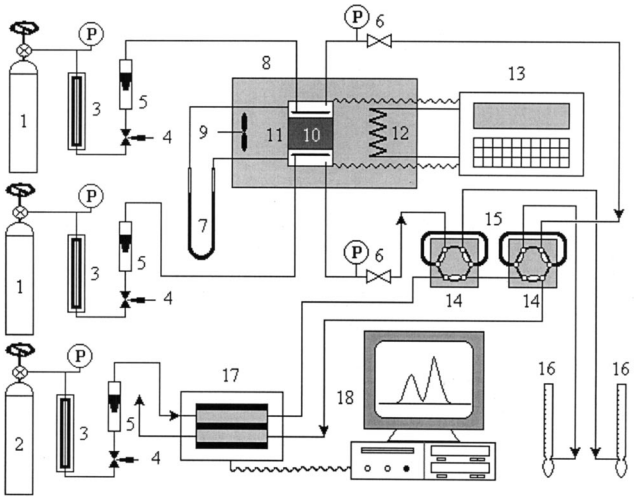

Figure 3. Flow sheet of experimental setups.

1. cylinders of diffusion gases; 2. cylinder of carrier gas; 3. filters; 4. needle valves; 5. rotameters; 6. BPRs; 7. U-tube manometer; 8. GC oven; 9. propeller; 10. catalyst pellet; 11. diffusion cell; 12. heater; 13. temperature detecting and controlling unit; 14. six-port valves; 15. sampling tubes; 16. soap-film flowmeters; 17. 3380 Varian GC; 18. computer with data processing system.

responding six-port valve after the system had reached steady state. Since the two sample tubes could be loaded simultaneously, the interval between the two sample injections was very short on the premise that the signals are able to be separated in the gas chromatograph. This arrangement, wherein the two six-port valves were connected in series, could make sure the sampling from the two compartments was taken at the same time. A computer with a data-processing system was used to deal with the chromatographic data. The gas flow rates from the compartments were measured by two soap-film flow meters.

Pellet molding

The amount of Ni/Al_2O_3 catalyst powder selected was put into a stainless steel ring that was 10 mm in thickness (the inner diameter was 15.8 mm) and compressed into a pellet, leaving about two equal-sized spaces on the two sides of the pellet. Molding pressure was set at 12 MPa in order to secure the seal between the two compartments. This unit was used as a diffusion cell after it had been sealed at both ends. The leak test was initially performed by using methane as a probe molecule. The reduction temperature was slowly raised to 200°C and kept there for about 24h. After the diffusion cell had cooled down to room temperature, the leak test was performed once again. The pellet surfaces exposed to the two compartments were polished so that the surface and the interior part of the pellet had the same porous structure.

Wicke-Kallenbach system

The diffusion cell was basically a standard Wicke-Kallenbach system except for the modification to the structure of the sweeping gas distributor. The gas was introduced into the compartment by way of a distributor, a loop of tubing with small holes of a sweep angle to the pellet surface. The pellet surfaces were swept by swirling gas streams with a relatively high flow rate at the holes. The temperature was controlled within a 0.5°C range by the GC oven. The symmetric length of tubing was used on both sides to achieve the pressure balance between the two sides. The tubing volume was also minimized to decrease the time lag in the gas sampling and concentration measurements.

Table 1. Characteristics of the Catalyst Pellet

ρ_P (kg/m^3)	ρ_S (kg/m^3)	d_{Hg} (nm)	ϵ	H (mm)
1730.0	2638.1	96.0	0.345	3.84

Selection of gas mixtures, experimental conditions, and porous catalysts

Nitrogen, carbon monoxide, carbon dioxide, helium, argon, methane, ethane, and propane were used in the experiment. Nitrogen (99.99% pure), carbon monoxide (99.90% pure), carbon dioxide (99.99% pure), helium (99.99% pure), and argon (99.99% pure) were purchased from the Tianjin Oxygen Company. Methane (99.99% pure), ethane (99.9% pure), and propane (99.9% pure) were supplied by the Yanshan Petrochemical Company. Those gases were combined into dozens of binary gas mixtures. The experiment was performed at 322.7 K and atmospheric pressure.

The catalyst particles used for molding were 0.125–0.150 mm in size. The characteristics of the catalyst pellet are given in Table 1. Those data were not measured until all the experiments of diffusion over the pellet had been finished. The pore-size distribution was measured by using mercury porosimetry and are displayed in Figure 4. The proportion of macropores formed by the molding of pellets is so small that the pore-size distribution could be considered to be monodisperse.

Results and Discussion

First, the yardstick sizes created by various gas species diffusing in the catalyst pellet were calculated by using Eq. 7, where the mean free path was procured by Eq. 2. The results are given in Figure 5. The figure shows that the yardstick size

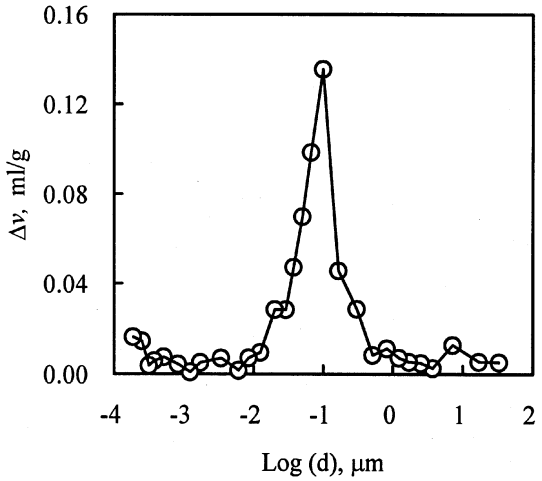

Figure 4. Pore-size distribution of the catalyst pellet.

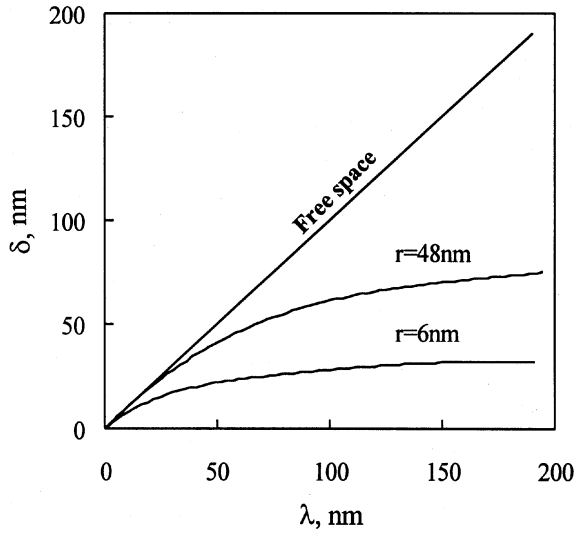

Figure 5. Yardstick size as the function of the mean free path and pore structure.

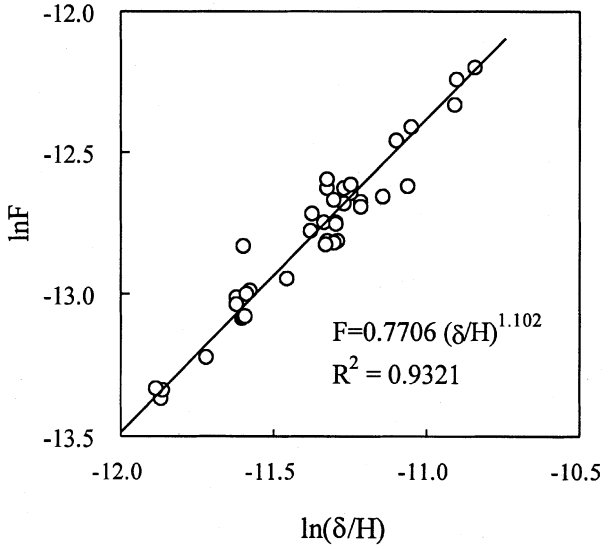

Figure 6. Variation of dimensionless flux with yardstick size.

is proportional to the mean free path by any means. However, the proportional relation is strongly influenced by the pore size of the catalyst pellet. For a given species, the average step length is affected by the pore diameter, as the pore wall restricts the free movement of the molecules and reduces the step length accordingly. The larger ratio of the mean free path to the pore diameter means the pore size has a greater influence on the yardstick size, just as the pore size does on the effective diffusion coefficient.

As shown in Figure 5, if the pore radius were to be decreased from 48 nm (the average pore radius of the catalyst pellet in this paper) to 6 nm, the yardstick size would be greatly decreased with respect to the same mean free path. Obviously, this is mainly due to the influence of pore size. With the increase in the mean free path for a specific pore system, the ratio of the mean free path to the pore diameter is increased, which leads to a further intensified restriction by the pore walls. However, if the pore diameter is increased for a specific mean free path, the pore effect on the average step length will be reduced. The pore effect will stop functioning, as the pore size is large enough to make sure that little restriction on molecular movement exists in the pores. The diagonal in Figure 5 represents this phenomenon. In this case, the yardstick size is the mean free path itself. The influence of pore walls on the average step length in the pores is too weak to be considered, so no modification on the mean free path is needed to acquire the yardstick size. This just corresponds to the molecular diffusion region without the influence of the pore walls.

This is in very good agreement with what is demonstrated in pore diffusion. When the ratio of the mean free path to the pore size changes from small to large, the transition from the molecular diffusion region to the Knudsen diffusion region also occurs. This shows that using the yardstick to measure the actual diffusion distance in the pores (as is done in this article) reflects the same mechanism as the gas diffusion process in the porous system.

It is worth noting that the yardstick size will become independent of the mean free path when the pore diameter is small enough. In this situation, the methodology developed here will fail, as a narrow measurement scale cannot result in an accurate fitting of the established model and the fractal dimension, thus compromising the reliability of the model's predictions. The variation in the yardstick size with the ratio $\lambda/(2\bar{r})$ can be broken into three regions compatible with pore diffusion, as illustrated in Table 2.

As for the experimental investigation, the molar flow rate together with concentration difference was measured for each binary gas mixture at 322.7 K and atmospheric conditions, so that the diffusion flux was found accordingly.

The dimensionless diffusion flux was calculated by Eq. 16 in terms of the experimentally measured diffusion flux, the physical properties of gas mixtures, and the operational temperature and pressure. The results are illustrated in Figure 6. Visual observation shows that the prediction performed by the model equation agrees well with the experimental points, and the differences are reasonable. The fractal dimension was obtained by fitting Eq. 18 with the experimentally determined data of dimensionless flux vs. calculated yardstick sizes (38 points altogether), the value of which was 1.102. The av-

Table 2. The Effect of Pore Size on the Yardstick Size

$\lambda/(2\bar{r})$	Small	Moderate	Large
Pore-size effect	Slight	Moderate	Strong
Yardstick size	The mean free path	The modified mean free path	Determined by pore size only
Scale range	Pretty large	Fairly large	Small
Model's Validity	Pretty good fitting	Fairly good fitting	Poor fitting, not recommended

Table 3. Variation of Orientation Factor $B_{\pi/2}(d_F)$ with Fractal Dimension, d_F

d_F	1.00	1.06	1.08	1.10	1.12	1.14	1.20	1.30
$B_{\pi/2}(d_F)$	0.7854	0.7764	0.7735	0.7706	0.7678	0.7650	0.7567	0.7434

erage relative deviation was only 5.7% with respect to the flux.

The fractal dimension of gas diffusion trajectories, d_F, is the only model parameter here. Because the orientation factor $B_{\pi/2}(d_F)$, as shown in Eq. 14, is the function of the fractal dimension, d_F, its variation with the fractal dimension has to be taken into account in the fitting process in light of Eq. 17 or 18. Therefore, when the equation is used for the linear fitting, $B_{\pi/2}(d_F)$ has to be adjusted to the right value. The values of $B_{\pi/2}(d_F)$ at different d_F are listed in Table 3. The visual observation and the average deviation show that the model agrees with the experimental data very well, and the obtained fractal dimension is in the reasonable range.

According to the model assumption presented in the section on the mathematical model, the fractal dimension, d_F, represents the irregularity of the gas diffusion trajectories in the porous system. In reality, it is the average outcome of the individual diffusion trajectories. This is because this average fractal dimension includes both topological and geometrical information, due to the built-in characteristics of gas diffusion across catalyst pellets. The diffusion of the molecules through the pores is limited by the reduced energy requirement. This implies that not all parts of the porous system are the same with respect to gas diffusion, and the trajectories of gas diffusion are the channels with the reduced resistance. The fractal dimension fitted by experimental data of gas diffusion is the devious measure of "effective" channels instead of all possible ones. Although this integrated characterization of pore structure does not provide a clear-cut picture that shows the geometrical and topological structures separately, it proves useful in a number of practical applications. For instance, West et al. (1997), Enquist et al. (1998), and Gillooly et al. (2001) reported fractal models that simulated the transport of nutrients and excretions in the vascular systems of living bodies. The reduced energy requirement to distribute the flux of materials was among the model assumptions based on the actual transport process in living organisms. Therefore, the integrated information of pore characterization of this type was needed in order to predict the transport process.

As far as the yardstick size is concerned, Coppens and Froment (1994) used effective molecular diameters to measure the actual pore length. This idea was taken from the measurement of the inner surface area proposed by Avnir and his coworkers (1984). The fractality of the surface could be detected by measuring the surface area with molecules of different sizes. As a matter of fact, the different-sized molecules crawl on the uneven surface, so the surface irregularity can be felt by means of this close physical touch. However, as for the molecular movement within the pores, molecules are jumping on their way from one end to the other. Unlike the measurement of the inner surface, those molecules do not touch anywhere on the surface, but only at some limited points. And each step between two consecutive collisions is

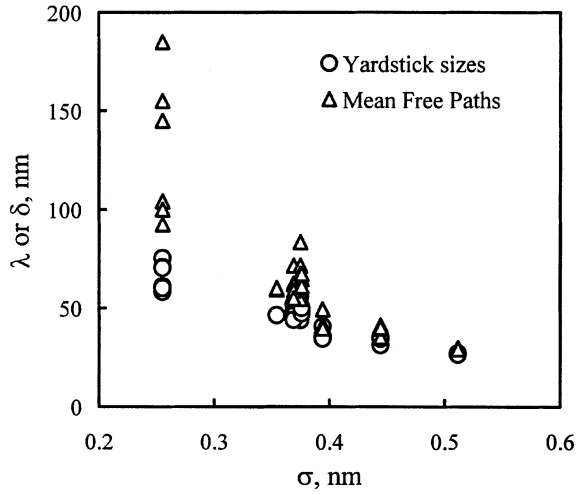

Figure 7. Variation of the mean free path and yardstick size with effective molecular diameter.

straight. So the irregularity of the diffusion trajectory with respect to the molecular movement in a pore must be reduced compared with that of the pore surface itself. Take the porous catalyst studied in this contribution as an example. The surface fractal dimension, D_S, of the catalyst determined by mercury intrusion is 2.86, which corresponds to 86% volume-filling (Zhang and Li, 1995). But the fractal dimension of the trajectory with respect to gas diffusion is only 1.102, which represents about 10% plane filling.

On the other hand, the effective molecular diameter is not proportional to the yardstick size or the mean free path. Figure 7 gives the differences between the yardstick size and the mean free path and the effective molecular diameters for various gases in the present study. These differences do not have a one-to-one relationship, because the mean free path depends on the overall properties of gas mixtures instead of those of individual ones. Besides, the difference between the effective molecular diameter and the yardstick size or the mean free path can be up to two orders of magnitude.

If the traditional treatment based on the tortuosity factor is used, then the rearrangement of Eqs. 15a and 15b leads to

$$N_{AZ} = \frac{PD_{AB}\epsilon_p\overline{Q}}{R_gT\left(\sqrt{M_A/M_B}-1\right)H}\cdot\frac{1}{\tau} \qquad M_A \neq M_B \quad (19a)$$

$$N_{AZ} = \frac{P\epsilon_p(y_{A0}-y_{AH})}{R_gT\left(1/D_{AB}+1/\overline{D}_{kA}\right)H}\cdot\frac{1}{\tau} \qquad M_A = M_B \quad (19b)$$

Comparing Eq. 19 with Eq. 15, the following relationship is attained:

$$\tau = \frac{1}{B_{\pi/2}(d_F)}\cdot\left(\frac{\delta}{H}\right)^{1-d_F}. \qquad (20)$$

Variable analyses of Eq. 20 predict that the traditionally defined tortuosity factor is relevant to the pore structure, the involved diffusion species, and operational temperature and

pressure. This agrees well with what was demonstrated by Satterfield (1970), where both "length factor" and "shape factor" were included in the tortuosity factor. Although the same influential factors are considered, the two treatments describe the problem from different angles. Nonetheless, since the influence of the tortuous degree in the pore axial and radial directions was represented by two parameters in the former treatment, the introduction of one more adjustable parameter made the problem even more complicated. Quantitatively, the tortuosity factor is defined as the ratio of the actual distance molecules travel across the pellet to its geometric thickness

$$\tau = \frac{L}{H} \tag{21}$$

By comparing Eq. 21 with Eq. 20, we see that the actual distance traversed by molecules with regard to gas diffusion in porous catalyst pellets is

$$L = \frac{1}{B_{\pi/2}(d_F)} \cdot \delta^{1-d_F} H^{d_F} \tag{22}$$

Here the influential factors, such as the tortuous degree of trajectories, pore size, physical properties of gas mixtures, operational temperature, and pressure, have all been included. In practical applications, the tortuosity factor with respect to a porous catalyst was attained by averaging a number of experimentally determined tortuosity factors for various diffusion species and/or under different operational temperatures and pressures. Up to now, the tortuosity factor measured by experiment has been typically in the range from a little bit higher than 1 to 16, depending on many factors such as the structural properties of the porous media, the experimental method, and even the theoretical treatment. So far, few researchers have noticed that even diffusion species themselves affect the value of tortuosity factors.

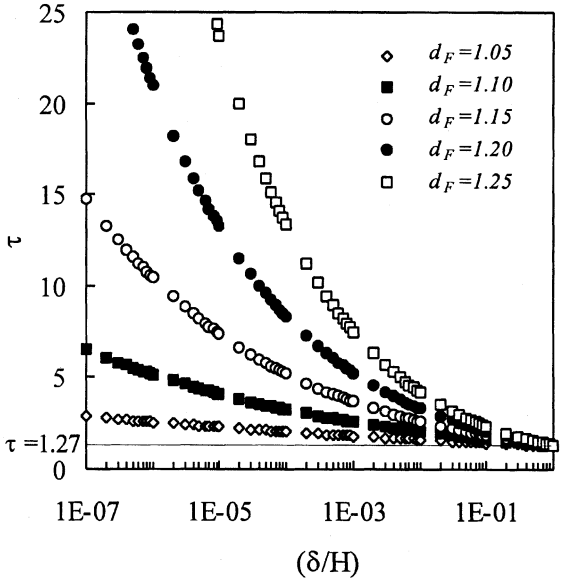

Figure 8. Tortuosity factor as a function of yardstick size for various fractal dimensions.

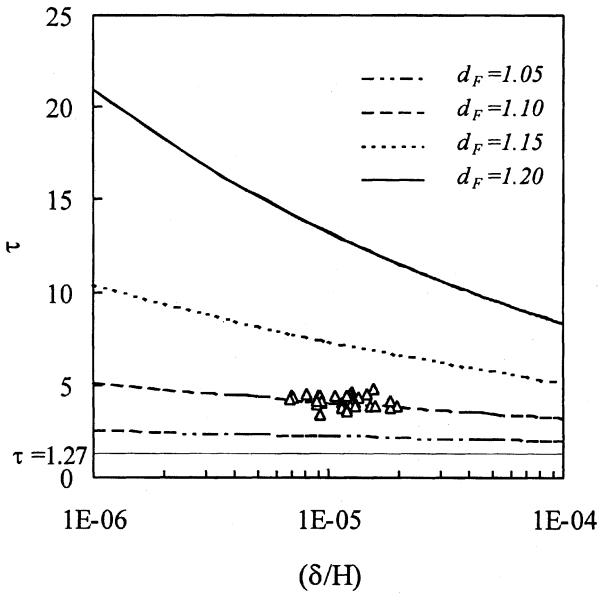

Figure 9. Comparison between measured tortuosity factor and its prediction by Eq. 20.

The tortuosity factor can be predicted through Eq. 20. Figure 8 presents the tortuosity factor over a wide range of dimensionless yardstick sizes with regard to different fractal dimensions. Since the dimensionless yardstick size is the ratio of two length scales, we can consider it to be a relative scale. The tortuosity factor obtained in each run of our experiments is given in Figure 9, which shows that the experimental points (open angles) fit in with Eq. 20 quite well. The methodology established in this article is especially significant when the scale range is large or the tortuous degree of the system is remarkable. The method based on the average tortuosity factor is only a simple approximation, which will fail when the discussed scale range is extensive due to the large difference between tortuosity factors across it. If the tortuous degree is large, the method based on the average tortuosity factor will also result in significant deviation, even if the discussed scale range is small. The prediction of Eq. 20 shows that the tortuosity factor can vary from about 1.27 to over 25 for not very tortuous porous systems. For a fixed pore structure, the tortuosity factor depends on the relative scale, δ/H.

The pellet size of ordinary catalysts is determined by the process and reactor where it is to be used. Considering the increase in diffusion resistance with particle size, the upper limit of catalyst pellets used in packed beds is 1/2 in. in diameter. But for fluidized beds, smaller particles are likely to be entrained. The particle size has to be over 20 μm in diameter (Satterfield, 1970). As far as porous inorganic membranes are concerned, modification is usually made for efficient gas separations and reactions leading to a thin layer on the very top of the membrane. The top-layer, a major part where diffusion resistance through the membrane is concerned, occurs in a wide range of thicknesses from nanometers to micrometers (de Lange et al., 1995; Soria, 1995; Saracco et al., 1999). The pore size of both catalyst pellets

and porous inorganic membranes may range from several angstroms up to micrometers (Satterfield, 1970; de Lange et al., 1995; Soria, 1995; Wegner et al., 1999; Mezedur et al., 2002). The upper limit of the yardstick size is the mean free path itself. It should be smaller than 200 nm according to the mean free path of hydrogen at ambient pressure and temperature. On the basis of the preceding information and analysis, the relative scale for both porous catalysts and membranes ranges from 10^{-7} to 1, as shown in Figure 8. It is evident that the relative scale for membranes is larger compared to catalyst pellets. The prediction performed by Eq. 20 shows that the tortuosity factor for catalyst pellets must be larger than that for membranes because of the relative scale difference, which is in fairly good agreement with the existing experimental results in the literature. The typical values of the tortuosity factor are $2 \sim 6$ for catalyst pellets and $1 \sim 2$ for porous membranes (Satterfield, 1970; Langhendries and Baron, 1998; Salmas and Androutsopoulos, 2001; Mezedur et al., 2002). Qualitatively speaking, this implies that the prediction by Eq. 20 is valid for both ordinary catalyst pellets and porous membranes. The restriction imposed by the values of tortuosity factors implies that the fractal dimension is unlikely to exceed 1.20 for both ordinary catalyst pellets and membranes.

Finally, it is worth mentioning here that the catalyst pellet investigated in this article has only a monodisperse pore structure. Both theoretical and experimental results have demonstrated that the mathematical model and methodology developed in this contribution are quite satisfactory. Regarding the catalyst pellets with macro–micro distribution (or bimodal porous structure), the methodology developed in the present study has to be modified further. The research work in this respect will be reported in a separate article where the mathematical model will be derived based on stochastic analysis.

Conclusions

A mathematical model and the methodology were developed for predicting the diffusion flux of binary gas mixtures in porous media. The model was developed based on the fractal analysis of the actual diffusing distance of gas diffusion in porous media, in which the diffusing trajectory of gas molecules was represented by fractal curves. As the only model parameter, *the fractal dimension of diffusing trajectories*, d_F, was used to measure the tortuous degree of pore structure with respect to gas diffusion. In addition, a yardstick was devised as the average step length to measure the actual diffusing distance of gas molecules in porous media. Starting with the mean free path and the mechanism of pore diffusion, the equation evaluating the yardstick size, δ, was deduced. It was shown that δ could be estimated if variables like pore size, diffusion species, temperature, and pressure were known.

The molar flow rate, together with the concentration difference, was measured for 19 groups of binary gas mixtures in a steady-state Wicke-Kallenbach diffusion cell molded with 3.84-mm catalyst pellet. Thus, the diffusion flux was determined. By fitting the experimentally determined flux with the model equation, the fractal dimension of diffusion trajectories was attained, that is, $d_F = 1.102$. It showed that the model prediction was in fairly good agreement with the experimental results with an average deviation of 5.7%. The fractal characterization of gas diffusion in porous media was experimentally affirmed. The model was very satisfactory with respect to the monodisperse porous catalyst pellet investigated in the article.

Unlike the traditional treatment that lumped all the possible influencing factors into the tortuosity factor, the methodology developed here used another parameter, the yardstick size, to account for the effect of pore size, diffusion species, temperature, and pressure on diffusion flux. The effect of pore size on the yardstick size was just the same as that demonstrated for pore diffusion. This showed that the measurement of actual pore length conforms to the mechanism of pore diffusion. Because the molecules jumped across the pore step by step, the yardstick size was claimed to be more appropriate than the effective molecular diameter in measuring the actual pore length with regard to gas diffusion in porous media. Thus, the tortuous degree of diffusing trajectory is much less than that of the pore surface. A detailed comparison with the traditional treatment in light of the tortuosity factor demonstrated that the model and methodology established in this article would be especially significant for very tortuous pore systems. In addition, according to an analysis of experimental data in the literature, the model can also apply to gas diffusion in membranes.

Acknowledgments

The authors acknowledge the financial support of the National Natural Science Foundation of China (NSFC) under Grant No. 20076033. Baoquan Zhang also thanks the Ministry of Education (MOE) for providing a senior fellowship grant.

Notation

d = pore diameter, m
d_F = fractal dimension of gas-diffusion trajectories in porous catalysts
D_{AB} = binary molecular diffusivity, m^2/s
D_{eff} = effective diffusion coefficient, m^2/s
D_K = Knudsen diffusion coefficient, m^2/s
D_p = diffusion coefficient in pore, m^2/s
d_{Hg} = average pore diameter by mercury intrusion, m
k_B = Boltzmann constant, J/K
$f(r,\Omega)$ = pore distribution function, m^2/m^3
F = dimensionless diffusion flux defined by Eq. 16
H = pellet length, m
L = actual distance traversed by molecules in diffusion, m
L_0 = projection of actual diffusion trajectory, m
M = molecular weight, kg/kmol
N_{Ap} = pore diffusion flux of A along moving direction, $mol/m^2 \cdot s$
$(N_{AZ})_p$ = pore diffusion flux of A along Z-direction, $mol/m^2 \cdot s$
N_{AZ} = diffusion flux of A on the whole pellet along Z-direction, $mol/m^2 \cdot s$
n = number of moles
P = total pressure, Pa
p = partial pressure, Pa
R = correlation coefficient
R_g = gas constant, $J/mol \cdot K$
r = pore radius, m
$\bar{r}$ = average pore radius, m
S = cross-sectional area, m^2
T = temperature, K
V = volume, m^3
v = specific volume, cm^3/g
X,Y = coordinate axes

y = concentration in mole fraction
Z = coordinate axis parallel to the diffusion

Greek letters

β = quantity defined in Eq. 8
δ = yardstick size, m
λ = mean free path, m
ϵ = porosity of catalyst pellet
ρ_p = bulk density of catalyst pellet, kg/m^3
ρ_S = solid density of catalyst pellet, kg/m^3
σ = effective diameter of molecule, m
σ_{ji} = mean effective diameter of molecules j and i defined as $(\sigma_j + \sigma_i)/2$
τ = tortuosity factor

Subscripts

A, B, ii_j = species A, B, i, j
F = fractal
G = point G
p = pore

Abbreviations

BPR = back-pressure regulator
GC = gas chromatograph
PSD = pore-size distribution

Literature Cited

Avnir, D., D. Farin, and P. Pfeifer, "Molecular Fractal Surfaces," *Nature*, **308**, 261(1984).

Avnir, D., ed. *Fractal Approach to Heterogeneous Chemistry*, Wiley, New York (1989).

Coppens, M.-O., and G. F. Froment, "Diffusion and Reaction in a Fractal Catalyst Pore—III. Application to the Simulation of Vinyl Acetate Production From Ethylene," *Chem. Eng. Sci.*, **49**(24A), 4897 (1994).

Coppens, M.-O., and G. F. Froment, "Diffusion and Reaction in a Fractal Catalyst Pore. I. Geometrical Aspects," *Chem. Eng. Sci.*, **50**(6), 1013 (1995a).

Coppens, M.-O., and G. F. Froment, "Diffusion and Reaction in a Fractal Catalyst Pore. II. Diffusion and First-Order Reaction," *Chem. Eng. Sci.*, **50**(6), 1027 (1995b).

Coppens, M.-O., and G. F. Froment, "Fractal Aspects in the Catalytic Reforming of Naphtha," *Chem. Eng. Sci.*, **51**(10), 2283 (1996).

Cunningham, R. E., and R. J. J. Williams, *Diffusion in Gases and Porous Media*, Plenum Press, New York (1980).

Cussler, E. L., *Diffusion, Mass Transfer in Fluid Systems*, 2nd ed., Cambridge Univ. Press, Cambridge (1997).

De Lange, R. S. A., J. H. A. Hekkink, K. Keizer, and A. J. Burggraaf, "Formation and Characterization of Supported Microporous Ceramic Membranes Prepared by Sol-Gel Modification Techniques," *J. Membr. Sci.*, **99**, 57 (1995).

Eldridge, B. D., and L. F. Brown, "The Effect of Cross-Sectional Pore Shape on Knudsen Diffusion in Porous Materials," *AIChE J.*, **22**, 942 (1976).

Enquist, B. J., J. H. Brown, and G. B. West, "Allometric Scaling of Plant Energetics and Population Density," *Nature*, **395**, 163 (1998).

Feng, C., and W. E. Stewart, "Practical Models for Isothermal Diffusion and Flow of Gases in Porous Solids," *Ind. Eng. Chem. Fundam.*, **12**(2), 143 (1973).

Fogler, H. S., *Elements of Chemical Reaction Engineering*, 3rd ed., Prentice Hall, Upper Saddle River, NJ (1999).

Gavrilov, C., and M. Sheintuch, "Diffusion-Controlled Rates in Fractal vs. Uniform-Pore Catalysts with Linear and Nonlinear Kinetics," *AIChE J.*, **43**, 1691 (1997).

Gillooly, J. F., J. H. Brown, G. B. West, Van M. Savage, and E. L. Charnov, "Effects of Size and Temperature on Metabolic Rate," *Science*, **293**, 2248 (2001).

Giona, M., W. A. Schwalm, A. Adrover, and M. K. Schwalm, "First-Order Kinetics in Fractal Catalysts: Renormalization Analysis of the Effectiveness Factor," *Chem. Eng. Sci.*, **51**(10), 2273 (1996).

Hollewand, M. P., and L. F. Gladden, "Modeling of Diffusion and Reaction in Porous Catalysts Using a Random Three-Dimensional Network Model," *Chem. Eng. Sci.,* **47**(7), 1761 (1992).

Jackson, R., *Transport in Porous Catalysts*, Elsevier, Amsterdam, The Netherlands (1977).

Johnson, M. F. L., and W. E. Stewart, "Pore Structure and Gaseous Diffusion in Solid Catalysts," *J. Catal.,* **4**, 248 (1965).

Karger, J., "The Random Walk of Understanding Diffusion," *Ind. Eng. Chem. Res.*, **41**, 3335 (2002).

Langhendries, G., and G. V. Baron, "Mass Transfer in Composite Polymer-Zeolite Catalytic Membranes," *J. Membr. Sci.*, **14**, 265 (1998).

Malek, K., and M.-O. Coppens, "Effects of Surface Roughness on Self- and Transport Diffusion in Porous Media in the Knudsen Regime," *Phys. Rev. Lett.*, **87**, 1255051 (2001).

Mandelbrot, B. B., *The Fractal Geometry of Nature*, Freeman, New York (1983).

Mezedur, M. M., M. Kaviany, and W. Moore, "Effect of Pore Structure, Randomness and Size on Effective Mass Diffusivity," *AIChE J.*, **48**(1), 15 (2002).

Michaels, A. S., "Diffusion in a Pore of Irregular Cross-Section—A Simplified Treatment," *AIChE J.*, **5**, 270 (1959).

Mougin, P., M. Pons, and J. Villermaux, "Catalytic Reactions at an Artificial Fractal Interface: Simulation with the 'Devil's Comb'," *Chem. Eng. J.*, **64**(1), 63 (1996a).

Mougin, P., M. Mos, and J. Villermaux, "Reaction and Diffusion at Artificial Fractal Interface: Evidence of New Diffusional Regime," *Chem. Eng. Sci.*, **51**, 2293 (1996b).

Nakano, Y., S. Iwamoto, I. Yoshinaga, and J. W. Evans, "The Effect of Pore Necking on Knudsen Diffusivity and Collision Frequency of Gas Molecules with Pore Walls," *Chem. Eng. Sci.*, **42**(7), 1577 (1987).

Sahimi, M., G. R. Gavalas, and T. T. Tsotsis, "Statistical and Continuum Models of Fluid-Solid Reactions in Porous Media," *Chem. Eng. Sci.*, **45**(6), 1443 (1990).

Salmas, C. E., and G. P. Androutsopoulos, "A Novel Pore Structure Tortuosity Concept Based on Nitrogen Sorption Hysteresis Data," *Ind. Eng. Chem. Res.*, **40**, 721 (2001).

Sapoval, B., J. S. Andrade, Jr., and M. Floche, "Catalytic Effectiveness of Irregular Interfaces and Rough Pores: the Land Surveyor Approximation," *Chem. Eng. Sci.*, **56**, 5011 (2001).

Saracco, G., H. W. J. P. Neomagus, G. F. Versteeg, and W. P. M. van Swaaij, "High-Temperature Membrane Reactors: Potential and Problems," *Chem. Eng. Sci.*, **54**, 1997 (1999).

Satterfield, C. N., *Mass Transfer in Heterogeneous Catalysis,* MIT Press, Cambridge, MA (1970).

Scott, D. S., and F. A. L. Dullien, "Diffusion of Ideal Gases in Capillaries and Porous Solids," *AIChE J.*, **8**, 113 (1962).

Sheintuch, M., and S. Brandon, "Deterministic Approaches to Problems of Diffusion-Reaction and Adsorption in a Fractal Porous Catalyst," *Chem. Eng. Sci.*, **44**, 69 (1989).

Sheintuch, M., "Selectivity and Deactivation of Diffusion-Limited Reactions in a Pore-Fractal Catalyst," *Ind. Eng. Chem. Res.*, **38**, 3261 (1999).

Sheintuch, M., "On the Intermediate Asymptote of Diffusion-Limited Reactions in a Fractal Porous Catalyst," *Chem. Eng. Sci.*, **55**(3), 615 (2000).

Soria, R., "Overview on Industrial Membranes," *Catal. Today*, **25**, 285 (1995).

Tien, C. L., and J. H. Lienhard, *Statistical Thermodynamics*, Hemisphere, Washington, DC (1979).

Wegner, K., J. H. Dong, and Y. S. Lin, "Polycrystalline MFI Zeolite Membranes: Xylene Pervaporation and its Implication on Membrane Microstructure," *J. Membr. Sci.*, **158**, 17 (1999)

West, G. B., J. H. Brown, and B. J. Enquist, "A General Model for the Origin of Allometric Scaling Laws in Biology," *Science*, **276**, 122 (1997).

Zhang, B. Q., and S. F. Li, "Determination of the Surface Fractal Dimension for Porous Media by Mercury Porosimetry," *Ind. Eng. Chem. Res.*, **34**, 1383 (1995).

Zhang, B. Q., X. F. Liu, and X. H. Ma, "Fractal Analysis in Heterogeneous Reactions: Characterization of Multi-Scale and Irregular Systems," *J. Tianjin Univer. Sci. and Technol.*, **16**(2), 5 (2001).

Manuscript received June 13, 2002, and revision received Apr. 3, 2003.